

Hysteretic memory effects in disordered magnets

Helmut G. Katzgraber¹ and Gergely T. Zimanyi²

¹*Theoretische Physik, ETH Zürich, CH-8093 Zürich, Switzerland*

²*Physics Department, University of California, Davis, California 95616, USA*

(Dated: November 11, 2018)

We study the return point as well as the complementary point memory effect numerically with paradigmatic models for random magnets and show that already simple systems with Ising spin symmetry can reproduce the experimental results of Pierce *et al.* where both memory effects become more pronounced for increasing disorder and return point memory is always better than complementary point memory.

PACS numbers: 75.50.Lk, 05.50.+q, 75.40.Mg, 75.60.Nt

Hysteresis is ubiquitous in nature: it occurs in interacting systems as a collective phenomenon, in most disordered systems, across first-order transitions, in magnetic systems, and in depinning phenomena, among others. It is also crucial for industrial applications: most notably hysteresis lies at the very foundation of the magnetic recording industry. Hysteretic systems are employed as recording media because they retain their state for a long period after a write operation: they exhibit memory. Many aspects of this memory effect have been studied: the long-time decay of information through the superparamagnetic decay¹ or how to optimize the signal-to-noise ratio by magnetic modeling, among others.

Because of the central importance of memory in recording media, other types of memory effects have been studied as well. Pierce *et al.* have investigated Co/Pt multilayer films by repeated cycling over the hysteresis loop.² The macroscopic magnetization returns to the same value cycle after cycle, a signature of a further type of memory. It is a profound question whether this memory comes about by the system returning to the same *microscopic* configuration: an effect dubbed “return point memory” (RPM), or whether it is exhibited only on the macroscopic level. Up to the groundbreaking work of Pierce *et al.*, it was not possible to address this question experimentally. By using an x-ray magnetic speckle microscopic technique which can indirectly resolve microscopic domain patterns, Pierce *et al.* found the presence of RPM for strong disorder, but no RPM for weak disorder. Furthermore, Pierce *et al.* studied a second type of memory: whether the system develops the reverse of the original configuration when the hysteresis sweep reaches the opposite magnetic field, called “complementary point memory” (CPM). They found that disorder influences CPM in the same way as RPM. In addition, they report that CPM appears to be smaller than RPM. However, the RPM–CPM difference does not exceed 10% and it is not clear whether the difference could have been caused by instrumental bias.

The experimental work of Pierce *et al.* spawned two theoretical studies to date. Deutsch and Mai have performed micromagnetic simulations using the Landau Lifshitz Gilbert (LLG) equations³ reproducing the above

memory effects. However, only few disorder realizations were considered, leading to large error bars. Furthermore, the difference between RPM and CPM was not much bigger than the error bars of the simulation. Finally, they suggest that the rotation of spins is primarily responsible for the RPM–CPM difference, i.e., scalar spins cannot cause the effect (in the absence of random fields). But since their model Hamiltonian contained numerous terms with several parameters, further clarification may be useful to determine which of these terms is the primary cause of the memory effects. Jagla also used the LLG approach, but for constrained soft scalar spins, subject to random fields.⁴ He reported seeing the memory effect and the RPM–CPM difference as well. However, no quantitative measure of the memory was given and the simulations were performed only at $T = 0$.

Therefore, the following challenges still remain to be understood: (i) What is the primary cause of the memory effect, or, equivalently, what is the minimal model that exhibits the memory effect? (ii) Does the memory effect persist at finite temperatures, since the thermal fluctuations have the potential to destroy microscopic correlations? (iii) What is the disorder dependence of the memory effects? (iv) Does the RPM–CPM difference convincingly exceed the error bars? To address these challenges, we have studied RPM and CPM in minimal, paradigmatic disordered spin models: spin glasses and random-field models. Equilibrium and close to equilibrium dynamical properties of spin glasses have been studied extensively over the years.^{5,6,7} However, far-from-equilibrium properties, such as their hysteresis, are much less understood. Recent studies characterized the hysteresis loop of the Edwards-Anderson spin glass (SG),⁸ the random field (RF) Ising model,⁹ and the Sherrington-Kirkpatrick model.¹⁰ While the RF model has been studied before, a comprehensive study with different models is still lacking. In this paper we address the above four challenges by studying disordered Ising-type models with and without frustration.

We first study the nearest-neighbor Edwards-Anderson Ising spin glass⁵ with the Hamiltonian

$$\mathcal{H}_{\text{SG}} = - \sum_{\langle i,j \rangle} J_{ij} S_i S_j - H \sum_i S_i \quad (1)$$

in which Ising spins $S_i = \pm 1$ lie on the sites of a square lattice of size $N = L^2$ with periodic boundary conditions. The measured quantities show essentially no size dependence past $L = 20$. The interactions J_{ij} are Gaussian distributed with zero mean and standard deviation σ_J . The simulations are performed by first saturating the system by applying a large external field H and then reducing H in small steps to reverse the magnetization. At zero temperature we use standard Glauber dynamics⁸ where randomly chosen unstable spins (pointing against their local field $h_i = \sum_{\langle j \rangle} J_{ij} S_j + H$) are flipped until all spins are stable for each field step. At finite temperatures we perform Monte Carlo simulations until the average magnetization is independent of the equilibration time of the Monte Carlo simulation for each field step. All results are averaged over 500 disorder realizations.

Pierce *et al.* captured the RPM and CPM in terms of overlaps of the spin configurations at different points of the hysteresis loop. Accordingly, we capture CPM and RPM with $q(H^*)$, the overlap of the spin configuration $S_i^{(0)}$ at a field H^* with the configuration $S_i^{(n)}$ at a field with the same magnitude $|H^*|$ after $n = 1/2$ (CPM) and 1 (RPM) cycles around the hysteresis loop, respectively:

$$q(H^*) = \frac{(-1)^{2n}}{N} \sum_{i=1}^N S_i^{(0)}[H^*] S_i^{(n)}[(-1)^{2n} H^*]. \quad (2)$$

The uniqueness of CPM and RPM is tested by $q'(H, H^*)$, the overlap between the spin configuration $S_i^{(0)}$ at H^* with a configurations $S_i^{(n)}$ at a field H after $n = 1/2$ (CPM) and 1 (RPM) cycles around the hysteresis loop:

$$q'(H, H^*) = \frac{(-1)^{2n}}{N} \sum_{i=1}^N S_i^{(0)}[H^*] S_i^{(n)}[H]. \quad (3)$$

To develop a physical picture, Fig. 1 illustrates configurations relevant for the CPM and RPM memory effects. The SG displays a large degree of CPM/RPM.

Figure 2 (left panel) shows $q(H^*)$ as a function of H^* for various temperatures. The RPM and CPM curves are indistinguishably close. The strong CPM can be attributed to the spin-reversal symmetry of the system: upon reversing all spins S_i and the magnetic field H , the Hamiltonian transforms into itself. Note that RPM is not perfect at $T = 0$ because of the nature of our spin updating. If unstable spins were sorted and not picked at random, RPM would be perfect at $T = 0$ (this is not the case if the ground state of the system is degenerate). The observation of a robust RPM and CPM memory is an answer to challenge (i), establishing the SG as a possible minimal model displaying memory effects just as in the experiments of Pierce *et al.* with no adjustable parameters. Also noteworthy is that the CPM and RPM are smallest around the (temperature-dependent) coercive field: as the number of equivalent spin configurations is the largest in that field region, the reversal process can

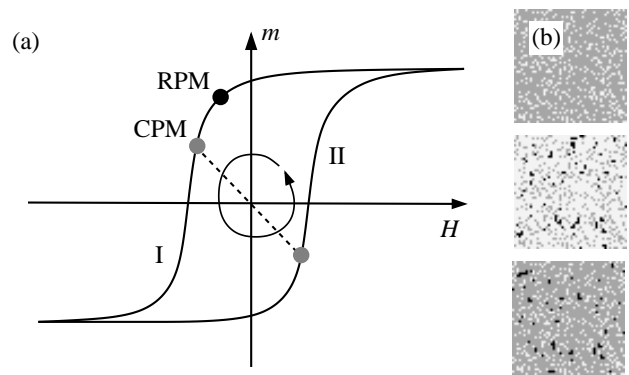


FIG. 1: (a) In CPM spin configurations on opposite branches I and II [$n = 1/2$ in Eq. (2)] of the hysteresis loop (gray dots) are compared, whereas in RPM a configuration on branch I [$\{S_i^{(0)}\}$ in Eq. (2)] is compared to itself after $n \in \mathbb{N}$ cycles around the loop (black dot). (b) Configurations for $|H^*| = 1.2$ for the two-dimensional Edwards-Anderson SG. Light pixels correspond to down spins, dark pixels correspond to up spins. Top: initial configuration at $H^* = -1.2$ (branch I). Center: configuration after a half cycle at $H = -H^*$ (CPM, branch II). Bottom: configuration at $H = H^*$ after one cycle around the hysteresis loop (RPM). The black pixels represent differences between the initial and final configurations.

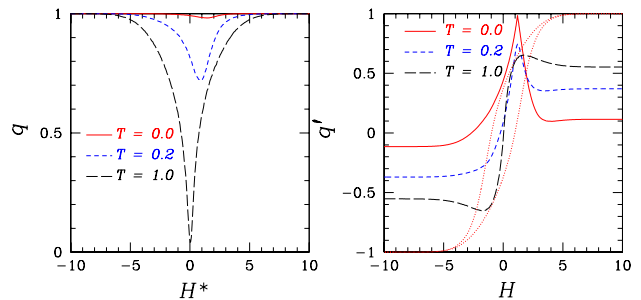


FIG. 2: (Color online) Overlaps for the 2D Edwards-Anderson SG. Left: Overlap q [Eq. (2)] for different values of H^* at different temperatures T . Right: Overlap q' [Eq. (3)] as a function of the applied field H for $H^* = -1.2$ (coercive field $H_c = -0.98$). The memory becomes more pronounced for $T \rightarrow 0$. Data for $\sigma_J = 1$. The dotted line represents the zero-temperature major loop.

evolve along many different paths. We also address the temperature dependence of the overlap, as raised at (ii). Figure 2 shows that the $T = 0$ CPM and RPM survive to finite T , even though it would be natural for the thermal fluctuations to wash out the memory at the microscopic level and convert it to a macroscopic memory only. In addition, the memory decreases with increasing temperature.

Figure 2 (right panel) shows $q'(H, H^* = -1.2)$ for various temperatures. The data show the uniqueness of CPM and RPM: the overlap function strongly peaks at $H = |H^*|$. Thus, the memory is not the result of a gradual slow buildup: there are large-scale spin rearrangements during the field sweep in frustrated systems,

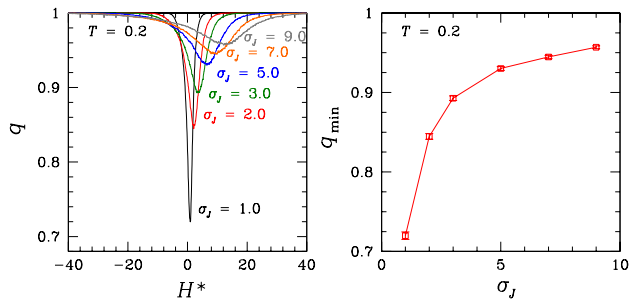


FIG. 3: (Color online) Left: overlap $q(H^*)$ for RPM and CPM (2D SG) as a function of H^* for different disorder strengths σ_J . Right: minimum value q_{\min} (at coercivity) of $q(H^*)$ as a function of disorder for RPM and CPM. Both sets of data show that the RPM and CPM increase with increasing disorder.

recreating the initial spin configuration only in the close vicinity of $H = |H^*|$. As above, CPM and RPM decrease with increasing temperature. The nonzero plateaus are caused by the measuring field $H^* = -1.2$ being different from the coercive field, where $M(H^*) \neq 0$.

Next, we address (iii), i.e., we explore the disorder dependence of both memory effects, since this aspect was an important element of the experiments of Pierce *et al.* Figure 3 (left panel) shows $q(H^*)$ as a function of the disorder σ_J at $T = 0.2$. The right panel of Fig. 3 shows $q(H^*)$ at coercivity as a function of σ_J . RPM and CPM are indistinguishable and visibly increase with increasing disorder, in good agreement with Ref. 2. The physical reason for this correlation is that for weak disorder, the energy landscape includes many comparable, shallow valleys, without a single optimal path. Therefore, during subsequent field sweeps, the system evolves along different paths, thus reducing the memory. In contrast, for stronger disorder, the energy landscape develops a few preferable valleys and the system evolves along these optimal valleys during subsequent cycling around the hysteresis loop. [The dips in $q(H^*)$ become broader with increasing disorder because the entire hysteresis loop broadens.] Finally, in relation to (iv) it is noted that in the SG RPM and CPM are indistinguishably close.

Next, we explore RPM and CPM, as well as the same four challenges in the 2D random field Ising model,

$$\mathcal{H}_{\text{RF}} = -J \sum_{\langle i,j \rangle} S_i S_j - \sum_i [H + h_i] S_i, \quad (4)$$

where $J = 1$ is a ferromagnetic coupling and the random fields h_i are chosen from a Gaussian distribution with zero mean and standard deviation σ_h . The main differences between the RF model and the Edwards-Anderson SG are that the RF model does not have frustration and does not have spin-reversal symmetry.

Figure 4 (left panel) shows both $q(H^*)$ for the RPM (dashed lines) and the CPM (solid lines) as a function of the field H^* for various temperatures. Concerning (i), this model also exhibits clear RPM, whereas CPM

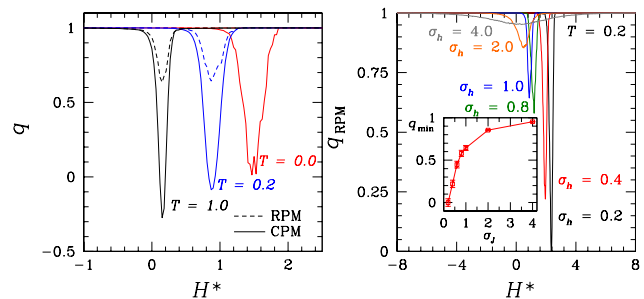


FIG. 4: (Color online) Left panel: Overlap q for RPM (dashed lines) and CPM (solid lines) for different temperatures for the RF model. The RPM is perfect at $T = 0$. For all temperatures the RPM is better than the CPM. In particular, for all temperatures the CPM is close to zero at coercivity suggesting that CPM is rather poor in this model. Right panel: Field dependence of $q(H^*)$ for RPM for different disorder strengths σ_h ($T = 0.20$). The RPM becomes better with increasing disorder at finite temperatures. The inset shows the disorder dependence of $q(H^*)$ for the RPM at coercivity.

is rather poor. Further, (ii) RPM is not washed out by thermal fluctuations at once, but is gradually weakened with increasing T .

Regarding (iv), the RF model deviates from the SG results and correlates with the experiments: in the RF model the RPM and CPM are different. The RPM is bigger than the CPM for all temperatures. This effect is due to the fact that the RF model does not have spin-reversal symmetry and therefore the spin configurations on the ascending branch do not correlate closely with the configurations on the descending branch. For intermediate-to-large values of the disorder the CPM is negligible and in the proximity of the coercive field the CPM correlation is in fact negative. In contrast, the RPM is large in the RF Ising model. In particular, at $T = 0$ the RPM is perfect due to the “no-crossing property” of the RF Ising model.¹¹ Figure 4 (right panel) shows (iii) $q(H^*)$ for the RPM for different disorder strengths σ_h at $T = 0.2$. RPM in the RF model also increases with increasing disorder, also illustrated in the inset: The overlap $q(H^*)$ at coercivity for RPM increases with increasing disorder. As for the SG, the memory effects increase due to the valleys in the energy landscape becoming more pronounced with increasing disorder.

In the RF model the CPM is always close to zero, whereas the RPM increases with increasing disorder (and is perfect at $T = 0$). Correspondingly, the RPM–CPM difference is large over much of the parameter space. These findings do not agree completely with the experimental results of Pierce *et al.* On the other hand the SG lacks the RPM–CPM asymmetry completely. Therefore we have explored whether a combination of the SG and the RF model might yield results comparable to the experiments: increasing memory with increasing disorder, as well as RPM being better than CPM. Thus we apply

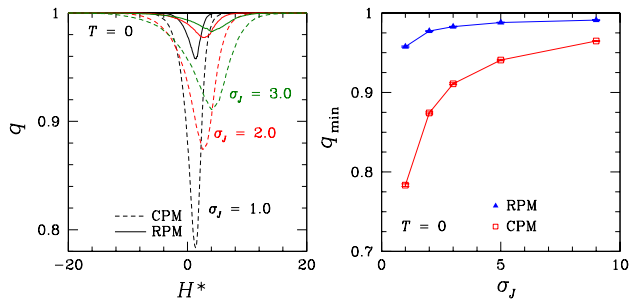


FIG. 5: (Color online) Left panel: Field dependence of $q(H^*)$ for RPM (solid lines) and CPM (dashed lines) for different disorder strengths σ_J ($T = 0$) for the SG+RF model [Eq. (5)]. The RPM is better than the CPM and both increase with increasing disorder. Right panel: Disorder dependence of $q(H^*)$ of the RPM and the CPM at coercivity. Both memory effects become better with increasing disorder, and RPM is larger than CPM, in good qualitative agreement with the experimental results of Pierce *et al.*

diluted random fields to the SG model:

$$\mathcal{H}_{\text{SG+RF}} = - \sum_{\langle i,j \rangle} J_{ij} S_i S_j - \sum_i [H + h_i] S_i. \quad (5)$$

The random bonds J_{ij} are chosen from a Gaussian distribution with zero mean and standard deviation σ_J . The random fields are randomly attached to only 5% of all sites, chosen from a Gaussian distribution with zero mean and standard deviation unity.

Figure 5 illustrates the results at $T = 0$ which persist well to finite T . The left panel of Fig. 5 shows $q(H^*)$ for both the RPM and the CPM as a function of H^* for different disorder strengths σ_J in the SG+RF model. The right panel of Fig. 5 shows the overlap q at coercivity for the RPM and the CPM. Both memory effects increase with increasing disorder and the RPM is larger than the CPM, in qualitative agreement with experimental results. These findings establish that the SG+RF model qualitatively reproduces all aspects of the Pierce *et al.* results.

In summary, we have simulated paradigmatic disordered spin models: the Edwards-Anderson spin glass, the random-field Ising model, and a spin glass with diluted random fields. We have found that (i) all three models

exhibit return point and complementary point memory. (ii) Both memory effects persist to finite temperatures. (iii) Both memory effects increase with increasing disorder. (iv) In the spin glass the RPM is always identical to the CPM because of the spin-reversal symmetry. In the RF Ising model the CPM is always close to zero because of the lack of spin-reversal symmetry. Finally, a spin glass where spin-reversal symmetry is broken with diluted random fields shows a moderate RPM–CPM difference, illustrating the sensitivity of the memory effects to the details of the models.

In relation to the experiments of Pierce *et al.*, one recalls that the films of Pierce *et al.* have strong out-of-plane anisotropy, restricting the orientation of the spins to being essentially perpendicular to the film. Thus, describing those films in terms of Ising Hamiltonians might be a reasonable approximation. Furthermore, since the dipolar interactions in these perpendicular films are antiferromagnetic, they introduce extensive frustration into the system, the key ingredient of the spin glass model. Finally, spins frozen in by shape anisotropies of a locally deformed environment, or by unusually large crystal field anisotropies, or possibly by frozen-in reversed bubbles, as reported by Davies *et al.* in Co/Pt multilayer films,¹² could all be the origin of random fields at a few percent of the sites. These considerations make it conceivable that all ingredients of the SG+RF model may be present in the Pierce *et al.* films. In addition, the SG+RF model agrees qualitatively with the experiments: RPM and CPM increase with increasing disorder and RPM is always more pronounced than CPM.

These results, together with the work by Deutsch and Mai, and that of Jagla show that a RPM-CPM asymmetry can only be obtained when the system's symmetry is broken. While Deutsch and Mai as well as Jagla break the symmetry *dynamically* using vector models with damped LLG dynamics, in this work we present an alternate avenue that breaks the symmetry *statically* using random fields. Thus in this work we present a plausible alternative which reproduces all aspects of the experiments within a minimal framework.

Acknowledgments We thank J. M. Deutsch, E. E. Fullerton, O. Hellwig, Kai Liu, R. T. Scalettar, and L. Sorensen for useful discussions.

¹ S. H. Charap, L. Pu-Ling, and H. Yanjun, IEEE Trans. Magn. **33**, 978 (1997).

² M. S. Pierce *et al.*, Phys. Rev. Lett. **94**, 017202 (2005).

³ J. M. Deutsch and T. Mai, Phys. Rev. E **72**, 016115 (2005).

⁴ E. A. Jagla, Phys. Rev. B **72**, 094406 (2005).

⁵ K. Binder and A. P. Young, Rev. Mod. Phys. **58**, 801 (1986).

⁶ A. P. Young, ed., *Spin Glasses and Random Fields* (World Scientific, Singapore, 1998).

⁷ N. Kawashima and H. Rieger (2003), (cond-mat/0312432).

⁸ H. G. Katzgraber *et al.*, Phys. Rev. Lett. **89**, 257202 (2002).

⁹ J. P. Sethna, K. Dahmen, S. Kartha, J. A. Krumhansl, B. W. Roberts, and J. D. Shore, Phys. Rev. Lett. **70**, 3347 (1993).

¹⁰ F. Pázmándi, G. Zaránd, and G. T. Zimányi, Phys. Rev. Lett. **83**, 1034 (1999).

¹¹ A. A. Middleton, Phys. Rev. Lett. **68**, 670 (1992).

¹² J. E. Davies *et al.*, Phys. Rev. B **70**, 224434 (2004).